Observations of large mass-independent fractionation occurring in MC-ICPMS: Implications for determination of accurate isotope amount ratios

Yang, Lu; Mester, Zoltán; Zhou, Lian; Gao, Shan; Sturgeon, Ralph E.; Meija, Juris

Publisher's version / Version de l'éditeur:
https://doi.org/10.1021/ac201795v
Analytical Chemistry, 83, 23, pp. 8999-9004, 2011-10-24

analytical chemistry

ARTICLE

pubs.acs.org/ac

Observations of Large Mass-Independent Fractionation Occurring in MC-ICPMS: Implications for Determination of Accurate Isotope Amount Ratios

Lu Yang,*[†,‡] Zoltán Mester,[†] Lian Zhou,[‡] Shan Gao,[‡] Ralph E. Sturgeon,[†] and Juris Meija[†]

[†]Institute for National Measurement Standards, National Research Council Canada, Ottawa, Ontario, K1A 0R6, Canada

[‡]State Key Laboratory of Geological Processes and Mineral Resources, China University of Geosciences, Wuhan, Hubei, 430074, China

ABSTRACT: Multicollector inductively coupled plasma mass spectrometry (MC-ICPMS) suffers large bias in isotope amount ratio determinations which has to be properly accounted for. The choice of the proper discrimination model is crucial. Over the last few decades, the exponential mass-bias correction model (Russell's law) has become a standard curriculum in isotope amount ratio measurements. In nature, however, isotopic fractionation that deviates significantly from the exponential model has been known for a long time. Recently, such fractionation was also observed in MC-ICPMS. This phenomenon is termed mass-independent fractionation. In this study, significant departure from the mass-dependent fractionation model is reported for germanium and lead with the most dramatic occurring for germanium-73 and lead-204 isotopes wherein, on average, close to a half percent bias was evidenced from the Russell's law.

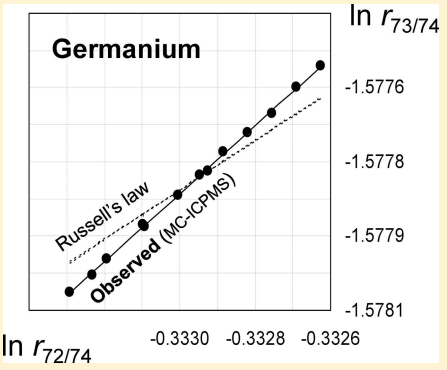

The phenomenon of mass-independent fractionation is a topic of revived interest in isotope measurement science.[1−3] It refers to any isotopic fractionation that does not adhere to the classical models wherein the magnitude of the fractionation has a smooth dependence on the nuclide mass. Mass-independent fractionation has been observed in various processes occurring in nature, most notably during the formation of ozone in the atmosphere.[4] In addition, mass-independent isotope effects in heavy elements are also detected in the laboratory during chemical separations.[5]

Similar to the processes occurring in nature, isotopic fractionation (discrimination) also occurs in mass spectrometers, the instruments used to determine isotope amount ratios. Natural and instrumental fractionation is commonly described with either linear or exponential functions, both of which apply only to the mass-dependent fractionation. With the prominence of the mass-independent processes in nature, a suggestion has been advanced that mass spectrometers might also, to some extent, discriminate various isotopes of an element in a manner that resembles mass-independent fractionation.[6] Compared to thermal ionization mass spectrometry (TIMS), multicollector inductively coupled plasma mass spectrometry (MC-ICPMS) suffers larger mass bias; proper correction of the mass bias is of the essence to generate accurate isotope amount ratios. Many mass-bias correction models were initially developed for use with TIMS systems.[7] The Russell mass-bias correction model, eq 1, remains the most popular:

$$R_{i,j} = r_{i,j}(m_i/m_j)^f \quad \text{or} \quad \ln(R_{i,j}/r_{i,j}) = f \times \ln(m_i/m_j) \tag{1}$$

For a given element E, $R_{i,j} = n(^iE)/n(^jE)$ is the (true) isotope amount ratio, $r_{i,j}$ is the observed (uncorrected) isotope amount ratio, f is the fractionation function, and m_i and m_j are the nuclide masses. When MC-ICPMS became commercially available in the 1990s, this correction model was adapted and has since become a standard curriculum.[7] Owing to the empirical nature of the Russell's model, many other mathematical expressions are in widespread use. These can be expressed in the following generalized power-law expression:[8]

$$\ln(R_{i,j}/r_{i,j}) = f \times (m_i^n - m_j^n) \tag{2}$$

where n is the discrimination exponent. One can show that eq 1 is a special case of eq 2 with $n \to 0$. This model comes with "adjustable" mathematical complexity by varying the value of n. In addition, each value of the fractionation exponent carries a designated name, which is often a source of confusion of its own. One thing, however, is common to all mass-bias models: they are designed to account for the smooth mass-dependent bias (with an additional assumption of identical mass bias for isotope amount ratios of both the calibrator and measurand). The application of these models to correct for instrumental bias for isotopes which display mass-independent discrimination can therefore produce inaccurate isotope amount ratios.

To date, only few studies have been devoted to critical analysis of deviations from the mass-dependent fractionation models in MC-ICPMS. Maximum deviations from the conventional exponential mass-bias models have been reported in the order of one part per thousand.[9−12] Owing to the comparatively large magnitude of the mass-bias in MC-ICPMS, this instrumental

Received: July 12, 2011
Accepted: October 24, 2011
Published: October 24, 2011

Table 1. MC-ICPMS Operating Conditions

Instrument Settings	
reflected forward power	1250 W
plasma Ar gas flow rate	15.0 L min^{-1}
auxiliary Ar gas flow rate	1.00 L min^{-1}
Ar carrier gas flow rate	1.020 L min^{-1}
sampler cone orifice (nickel)	1.1 mm
skimmer cone orifice (nickel)	0.8 mm
lens settings	optimized for maximum analyte signal
Data Acquisition Parameters	
scan type	static
Faraday cup configuration	see Table 2
mass resolution, $m/\Delta m$	~300
sensitivity	6.2 V for ^{72}Ge/ppm, 1.2 V/ppm for ^{201}Hg, 4.2 V/ppm for ^{92}Zr, 8.8 V/ppm for ^{208}Pb
blank signal	0.00016 V for ^{72}Ge, 0.003 V for ^{201}Hg, 0.0003 V/ppm for ^{92}Zr, 0.0002 V/ppm for ^{208}Pb,
signal integration time	33.55 s
number of integrations	1
cycles/blocks	10/3−4

platform is ideally suited to examine the mass-bias models. Thus, in this study, investigation of instrumental discrimination of Ge, Pb, and Hg isotopes within MC-ICPMS was conducted.

EXPERIMENTAL SECTION

Instrumentation. A Thermo Fisher Scientific Neptune (Bremen, Germany) MC-ICPMS equipped with nine Faraday cups and a combination of cyclonic and Scott-type spray chambers with a perfluoroalkoxy self-aspirating nebulizer (Elemental Scientific MCN50; Omaha, NE, USA) operating at 50 μL min^{-1} was used for all measurements. The plug-in quartz torch with sapphire injector was fitted with a platinum guard electrode. Low-resolution mode was used for all measurements. However, high mass-resolution was employed in all preliminary work to ensure absence of isobaric interferences. Optimization of the Neptune MC-ICPMS was performed daily as recommended by the manufacturer; typical operating conditions are summarized in Table 1. Typical signal intensities for all analyte solutions and the respective procedural blanks are shown in Table 1.

Reagents and Solutions. Nitric and hydrochloric acids were purified in-house prior to use by sub-boiling distillation of reagent grade feedstock in a quartz still. Environmental grade hydrofluoric acid was purchased from Anachemia Science (Montreal QC, Canada) and high-purity deionized water (18 MΩ cm) was obtained from a NanoPure mixed-bed ion exchange system fed with reverse osmosis domestic feedwater (Barnstead/Thermolyne; Iowa, USA). A 0.2 M solution of BrCl was prepared in a fume hood by dissolving 27 g of KBr (Fisher Scientific; Nepean ON, Canada) in 2.5 L of concentrated HCl followed by a slow addition of $KBrO_3$ (38 g) while stirring.

Reference materials with certified isotope amount ratios of lead (SRM 981, 982) were obtained from the National Institute of Standards and Technology (NIST; Gaithersburg MD, USA). Isotopic reference material for mercury (NIMS-1) was obtained from the National Research Council Canada (NRC-INMS; Ottawa ON, Canada). High-purity Ge was purchased from Sigma-Aldrich (w = 99.999%; Oakville ON, Canada).

Stock solutions of germanium (2500 μg g^{-1}) were prepared by quantitative dissolution of high-purity Ge metal in a mixture of HNO_3/HF followed by dilution with water. Stock solutions of SRM 981 and SRM 982 for Pb (1000 μg g^{-1}) were prepared by quantitative dissolution of Pb in dilute HNO_3 followed by dilution with water to result in a matrix of 2% HNO_3.

Sample Preparation and Analysis. Sample preparation was conducted in a Class-100 clean room. Solutions of 4 μg g^{-1} Ge and 0.75−1.0 μg g^{-1} Pb were each prepared in 2% HNO_3, separately, for determination of their isotope amount ratios. For Hg, replicate solutions of 500 ng g^{-1} Hg were prepared by diluting the stock in a solution of 2% HCl containing 1 mM BrCl. More details regarding the characterization of mercury and germanium can be found in our recent studies devoted entirely to these isotopic systems.[13,14]

Samples were introduced into the plasma in a self-aspiration mode at a flow rate of 50 μL min^{-1}. Intensities of analyte and internal standard isotopes and all other measured isotopes of interest (see below) obtained from corresponding blank solutions of 2% HNO_3, 1% HNO_3, and 1% HCl or 2% HCl, each containing 1 mM BrCl, were subtracted from those of all samples. Static runs were employed to simultaneously collect each set of isotopes of interest using the Faraday cup configurations shown in Table 2. Ten to thirteen measurements were made for each sample solution over a duration of 10−13 h. Data sets reported here were collected between November 2007 and January 2011.

Spectral Interferences. As no significant amounts of zinc or selenium were detected in the dilute solutions of Ge prepared from high purity metal, there was no need to correct for minor isobaric interferences from ^{70}Zn on ^{70}Ge or ^{74}Se on ^{74}Ge. No significant Si was found in the test solutions, confirming $^{40}Ar^{29}Si^+$ and $^{40}Ar^{20}Si^+$ interferences were not present. Potential polyatomic interferences from $^{36}Ar^{35}Cl^+$, $^{36}Ar^{36}Ar^+$, $^{36}Ar^{37}Cl^+$, $^{36}Ar^{35}Cl^+$, $^{36}Ar^{38}Ar^+$, and $^{36}Ar^{40}Ar^+$ on Ge isotopes were corrected for by subtracting intensities measured from the 2% HNO_3 solution used for sample preparation. In general, measured background intensities for Ga isotopes in the 2% HNO_3 solution were at least 3 to 4 orders of magnitude lower than those obtained from germanium samples, confirming insignificant contributions from Ar_2^+ or its associated polyatomic ions. Isotopes ^{195}Pt and ^{206}Pb were monitored using ion counters IC4 and IC5 during Hg measurements. Minor isobaric interferences from ^{196}Pt on ^{196}Hg, ^{198}Pt on ^{198}Hg, and ^{204}Pb on ^{204}Hg were subtracted on the basis of the intensities simultaneously measured on ^{195}Pt and ^{206}Pb. For this correction, the standard isotopic composition was assumed for both Pt and Pb.[14] However, the signal intensities for Pt and Pb in dilute solutions of NIMS-1 were on the order of 1000 counts/s and exerted no detectable influence on corrected Hg isotope amount ratios. Potential interference on ^{204}Pb by Hg was monitored during Pb measurements using the L3 Faraday cup (^{202}Hg signal). The intensity for ^{202}Hg from the Pb solution was found to be the same as that obtained with the 2% HNO_3 blank. Thus, no specific interference correction for ^{204}Hg on ^{204}Pb was necessary. Ion counters and Faraday cups were cross-calibrated in accordance

Table 2. MC-ICPMS Faraday Cup Detector Configuration

Faraday cup	L4	L3	L2	L1	C	H1	H2	H3	H4
Ge	(^{68}Zn)	(^{69}Ga)	^{70}Ge	(^{71}Ga)	^{72}Ge	^{73}Ge	^{74}Ge	^{76}Ge	
cup position, mm	72.500	55.467	34.790	15.808	0	15.546	34.777	69.966	
Hg	^{196}Hg	^{198}Hg	^{199}Hg	^{200}Hg	^{201}Hg	^{202}Hg	(^{203}Tl)	^{204}Hg	(^{205}Tl)
cup position, mm	42.060	26.500	16.650	7.280	0	6.800	16.500	26.000	35.950
Pb		(^{202}Hg)	(^{203}Tl)	^{204}Pb	(^{205}Tl)	^{206}Pb	^{207}Pb	^{208}Pb	
cup position, mm		26.112	16.450	7.168	0	6.800	16.320	25.700	

with the manufacturer's recommended procedures. No significant memory effect from Hg was evident when solutions of 2% HCl containing 1 mM BrCl as sample matrix and wash solutions were used; the ^{201}Hg signal (0.6 V for 500 ng g^{-1} Hg solution) was reduced to its baseline level (3 mV) within several minutes of washing. Data acquisition parameters are summarized in Table 1.

RESULTS AND DISCUSSION

The objective of this study is to investigate whether mass-independent fractionation (MIF) occurs in MC-ICPMS for isotope systems other than those reported previously (Nd[12], W[15], Cd[16]) and to ascertain the validity of the exponential mass-bias correction model. The three isotope-plot approach (known as the $\delta'-\delta'$ plot) has been successfully applied to delineate the nature of isotope fractionation. In general, adherence to any particular mass-bias model (eq 1-2) can be ascertained from the simultaneous instrumental drift of any three isotope signals (two isotope amount ratios).[17−21]

Deviations from the Mass-Bias Models. The bias between the true isotope amount ratio, $R_{i/j} = N(^iE)/N(^jE)$, and the instrumentally determined result, $r_{i/j}$, is commonly expressed as a ratio, $K_{i/j} = R_{i/j}/r_{i/j}$, termed the "mass-bias factor" for a given pair of isotopes (here, ^iE and ^jE). In general, mass-bias correction models express the mass-bias relationships between the various isotope pairs (of the same or differing elements). For two isotope pairs of an element E, say $^iE-^jE$ and $^kE-^jE$, the two mass-bias correction factors are presumed to be proportional to the mass ratio of the nuclides (eq 1) or to the power of mass difference of the nuclides (eq 2). Simple linear models have been often used in the past; however, we do not consider them here. In the logarithmic form, eq 2 (generalized power-law model) for two isotope pairs is as follows:

$$\begin{cases} \ln(R_{i/j}) - \ln(r_{i/j}) = f_{i/j}(m_i^n - m_j^n) \\ \ln(R_{k/j}) - \ln(r_{k/j}) = f_{k/j}(m_k^n - m_j^n) \end{cases} \quad (3)$$

To apply this model, an assumption of $f_{i/j} = f_{k/j}$ has to be made, regardless of the veracity of such an assumption. From here, the above mass-bias model leads to the following interpretation of the log−linear drifts of measured isotope ratios:

$$\ln(r_{i/j}) = \ln(R_{i/j}) - \frac{m_i^n - m_j^n}{m_k^n - m_j^n} \times \ln(R_{k/j}) + \frac{m_i^n - m_j^n}{m_k^n - m_j^n} \times \ln(r_{k/j}) \quad (4)$$

It is noteworthy that slopes of the above regressions do not depend on the absolute isotope amount ratios as the latter only offset the intercept of the above regression. In addition, the "predicted" slope depends only on the nuclide masses (and the chosen fractionation exponent, n). The above equation can thus be rewritten as follows:

$$\ln(r_{i/j}) = a + b \times \ln(r_{k/j}) \quad (5)$$

Log−linear regressions of two isotope ratios (three isotope plots) are obtained by simultaneously monitoring the isotope signals over a prolonged period of time, 10−15 h. This can yield three possible outcomes: (1) measurement results fall on the line in agreement with the conventional mass-dependent fractionation (eq 1); (2) data are correlated but fall on a line with a slope that differs from that of the "predicted" line or even forms a curve; (3) data are not correlated; i.e., they scatter nonsystematically, in which case instrumental artifacts are likely to be the major cause for the observed offsets.

The numerical value of the slope b (eq 5) is determined by two factors: (1) by the choice of the mass-dependent fractionation model, i.e., value of the fractionation exponent n, and (2) by the presence of mass-independent fractionation, i.e., $f_{i/j} \neq f_{k/j}$.

Isotopes of Germanium. Typical slopes generated in three-isotope plots and their respective "predicted" mass-dependent slopes are summarized in Figure 1. Slopes obtained for isotope ratios involving the ^{73}Ge deviate consistently and significantly from their respective theoretical values. For example, an average value of $b_{exp} = 0.61(4)$ is obtained for the slope ^{73}Ge−^{74}Ge vs ^{72}Ge−^{74}Ge slope whereas all conventional mass-bias models dictate a value of $b_{theor} = 0.50(1)$ ($n = -1...+2$). Similar results are obtained when the common denominator isotope is changed from ^{74}Ge to ^{70}Ge or ^{76}Ge.

Departures of the observed $\ln r_{i/j} - \ln r_{k/j}$ slope (b_{exp}) from the values prescribed by the model (b_{theor}) have an effect on the mass-bias corrected isotope ratios. According to eq 2, the mass-bias correction factors are related as follows:

$$K_{i/j} = K_{k/j}^b \quad (6)$$

If the experimental value of b, b_{exp}, differs from the model-prescribed value (b_{theor}), the following relative bias in the isotope amount ratio $N(^iE)/N(^jE)$ is introduced:

$$\frac{\Delta K_{i/j}}{K_{i/j}} = K_{k/j}^{(b_{exp} - b_{theor})/b_{exp}} \approx 1 + \frac{b_{exp} - b_{theor}}{b_{exp}}(K_{k/j} - 1) \quad (7)$$

The above data for ^{73}Ge−^{74}Ge vs ^{72}Ge−^{74}Ge with the average 20% discrepancy between the observed and "predicted" slopes lead to a half-percent relative bias in the mass-bias corrected isotope ratio of $N(^{73}Ge)/N(^{74}Ge)$ when $N(^{72}Ge)/N(^{74}Ge)$ is used as a calibrator ($K_{72/74} = 1.04$ was obtained in this study).

Anatomy of Deviations. Similar to the above Ge isotope study, Hg and Pb isotopic systems were evaluated. These measurements are summarized in Figures 2 and 3.

Three prominent features of the mass bias in the Neptune MC-ICPMS are apparent from this study. First, mass-independent

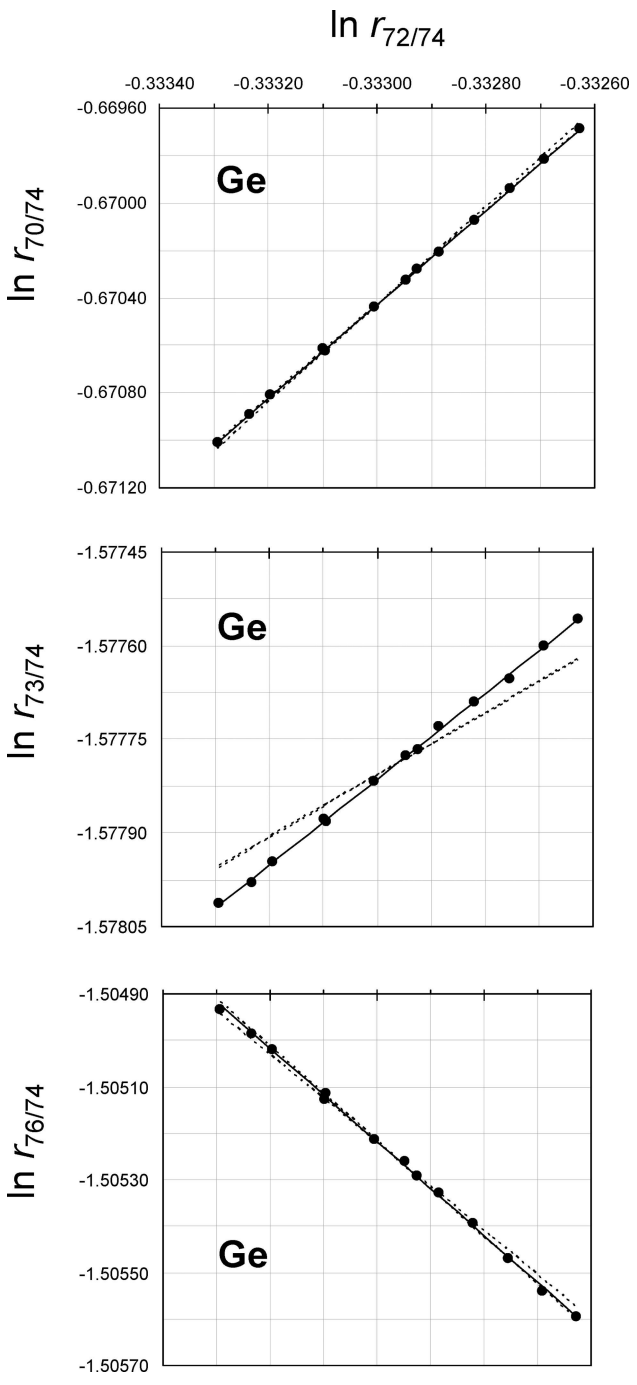

Figure 1. Typical three-isotope plots for germanium arising from measurements acquired over a 10−12 h period. Solid lines represent predicted mass-dependent fractionation as given by the eq 5 with $n = +2$ and -1 ($n \rightarrow 0$ for the Russell's model). All nuclide masses were obtained from the 2003 Atomic Mass Evaluation report.[22,23]

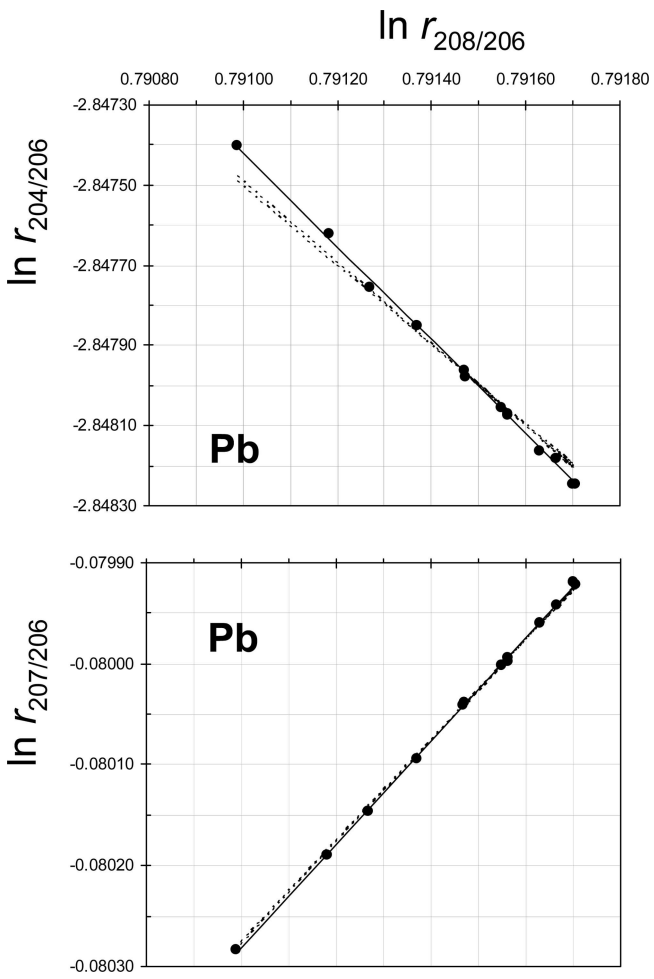

Figure 2. Typical three-isotope plot for Pb arising from measurements acquired over a 10−12 h period. Solid lines represent predicted mass-dependent fractionation as given by the eq 5 with $n = +2$ and -1 ($n \rightarrow 0$ for the Russell's model). All nuclide masses were obtained from the 2003 Atomic Mass Evaluation report.[22,23]

discrimination does occur in MC-ICPMS. The most striking deviation is evident for the isotope ^{73}Ge which amounts to a half-percent. Deviations of this magnitude have never been reported. Second, deviations from the Russell's correction model are not systematic over time. This is best exemplified with ^{73}Ge, ^{201}Hg, or ^{204}Pb where day-to-day variability of the apparent mass bias is significant (see Figure 3). This day-to-day variation is possibly due to different plasma conditions producing different mass bias. This is supported by the results of Shirai and Humayun[15] in their study of W isotopes, wherein different ICP cones produced varying degrees of fractionation behavior. Third, deviations from the exponential correction model are not systematic over the nuclide mass domain. That is to say, isotopes which show the largest deviations are not necessarily those with nonzero nuclear spin. Mercury isotopes ^{201}Hg and ^{204}Hg, for example, both show equally large deviations from the exponential model in reference to ^{202}Hg/^{198}Hg, which often amounts to 0.1%.[11] Likewise, deviations of ^{204}Pb/^{206}Pb from the Russell's model are significantly larger than those of ^{207}Pb/^{206}Pb (Figure 2). The observation of large mass-independent fractionation for Ge isotopes further confirms that traditional mass-bias correction models, such as Russell's law, are, in principle, not suitable for absolute isotope amount ratio measurements when MC-ICPMS is used.

It is known that the magnetic moment of the atomic nucleus plays a significant role in chemical reactions involving radicals[24−26] and, by association, many have embraced the hypothesis that departures of the mass-bias from the exponential model are also due to a nonzero magnetic moment in "odd" isotopes[12] (note that some isotopes with even mass number, such as deuterium, are also magnetic). Although significant mass-independent fractionation is

dx.doi.org/10.1021/ac201795v |*Anal. Chem.* 2011, 83, 8999–9004

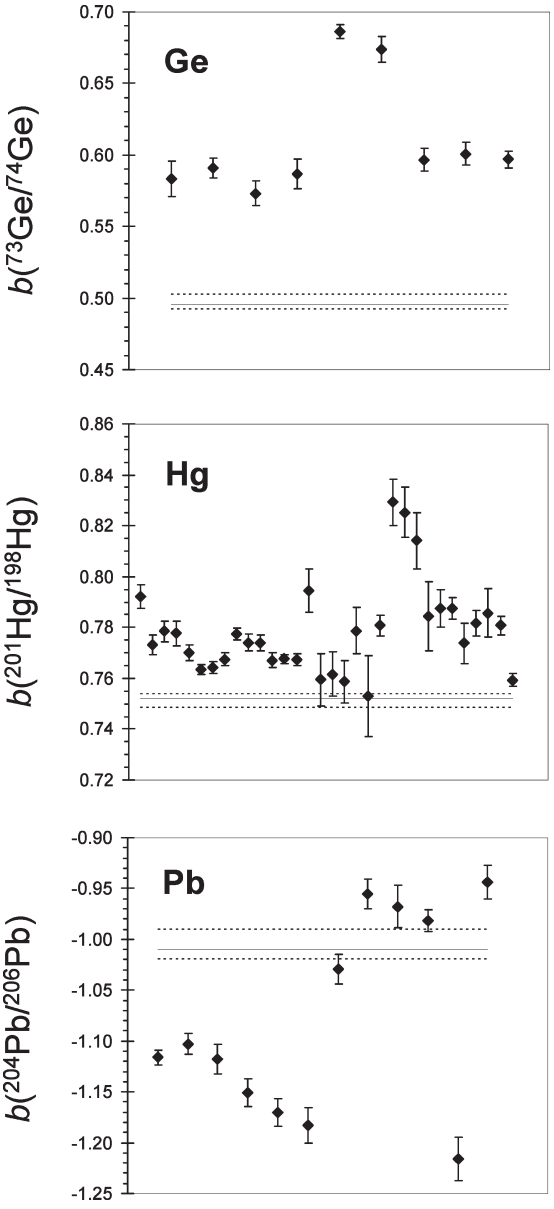

Figure 3. Time-series plot of the germanium, lead, and mercury isotope ratio regression slopes. Slope according to the Russell's model is shown as solid line ($n \rightarrow 0$, eq 5). Dotted lines correspond to the slopes of the generalized power-law model with $n = +2$ and -1 (eq 5). Isopte ratios $^{74}Ge/^{72}Ge$, $^{208}Pb/^{206}Pb$, and $^{202}Hg/^{198}Hg$ are used as reference, and uncertainties are given as $U = ku$ where $k = 1$.

indeed observed in MC-ICPMS for magnetic isotopes (for example, ^{73}Ge and ^{201}Hg), in this study, mass-independent fractionation is also observed for "even" isotopes (for example, ^{200}Hg and ^{204}Pb). Thus, mass-bias behavior of all isotopes cannot be divided into two distinct categories: one for all nonmagnetic nuclei and another for all magnetic nuclei. Rather, the magnitude of the observed departures is haphazard both in time and nuclide mass domains and is clearly not governed by the presence of the magnetic moment of the nuclides alone.

CONCLUSIONS

Recent interest in the mass-independent isotope fractionation induced by mass spectrometers has focused much attention on the likely cause of this effect (magnetic moment or nuclear field shift), whereas the potential impact of this phenomenon has escaped metrological scrutiny.[11] Herein, we report the largest deviations from the Russell's mass-bias model measured to date: for germanium-73 and lead-204, the deviation from the exponential model is, on average, close to a half percent when the $^{72}Ge-^{74}Ge$ or $^{206}Pb-^{208}Pb$ isotope pairs are used to correct for $N(^{73}Ge)/N(^{74}Ge)$ and $N(^{204}Pb)/N(^{206}Pb)$, respectively. This finding illustrates that the isotope amount ratio measurement results obtained using classical mass-bias models, such as Russell's law, need to be revisited. We also provide evidence that neither nuclear spin nor changes in nuclear volume can systematically account for the observed departures in the mass bias patterns; hence, the cause for these departures remains unknown. In this vein, the idea of tuning the MC-ICPMS not only for the highest sensitivity but also for the smallest mass bias remains an attractive alternative.[27]

AUTHOR INFORMATION

Corresponding Author
*E-mail: lu.yang@nrc-cnrc.gc.ca.

ACKNOWLEDGMENT

L.Z. and S.G. thank the State Key Laboratory of Geological Processes and Mineral Resources Foundation (Grant No. GPMR201106) and the Ministry of Education of the People's Republic of China (Grant No. B07039) for partial support.

REFERENCES

(1) Bergquist, B. A.; Blum, J. D. *Science* **2007**, *318*, 417–420.
(2) Sherman, L. S.; Blum, J. D.; Johnson, K. P.; Keeler, G. J.; Barres, J. A.; Douglas, T. A. *Nat. Geosci.* **2010**, *3*, 173–177.
(3) Epov, V. N.; Malinovskiy, D.; Vanhaecke, F.; Begue, D.; Donard, O. F. X. *J. Anal. At. Spectrom.* **2011**, *26*, 1142–1156.
(4) Thiemens, M. H.; Heidenreich, J. E., III *Science* **1983**, *219*, 1073–1075.
(5) Fujii, T.; Moynier, F.; Albarede, F. *Chem. Geol.* **2009**, *267*, 139–156.
(6) Vance, D.; Thirlwall, M. *Chem. Geol.* **2002**, *185*, 227–240.
(7) Yang, L. *Mass Spectrom. Rev.* **2009**, *28*, 990–1011.
(8) Maréchal, C. N.; Télouk, P.; Albaréde, F. *Chem. Geol.* **1999**, *156*, 251–273.
(9) Newman, K.; Freedman, P. A.; Williams, J.; Belshaw, N. S.; Halliday, A. N. *J. Anal. At. Spectrom.* **2009**, *24*, 742–751.
(10) Schmitt, A.-D.; Galer, S. J. G.; Abouchami, W. *J. Anal. At. Spectrom.* **2009**, *24*, 1079–1088.
(11) Meija, J.; Yang, L.; Sturgeon, R.; Mester, Z. *Anal. Chem.* **2009**, *81*, 6774–6778.
(12) Mead, C.; Johnson, T. M. *Anal. Bioanal. Chem.* **2010**, *397*, 1529–1538.
(13) Meija, J.; Yang, L.; Sturgeon, R. E.; Mester, Z. *J. Anal. At. Spectrom.* **2010**, *25*, 384–389.
(14) Yang, L.; Meija, J. *Anal. Chem.* **2010**, *82*, 4188–4193.
(15) Shirai, N.; Humayun, M. *J. Anal. At. Spectrom.* **2011**, *26*, 1414–1420.
(16) Schmitt, A. D.; Galer, S. J. G.; Abouchami, W. *J. Anal. At. Spectrom.* **2009**, *24*, 1079–1088.
(17) Hulston., J. R.; Thode, H. G. *J. Geophys. Res.* **1965**, *70*, 3475–3484.
(18) Young, E. D.; Galy, A.; Nagahara, H. *Geochim. Cosmochim. Acta* **2001**, *66*, 1095–1104.
(19) Galy, A.; Belshaw, N. S.; Halicz, L.; O'Nions, R. K. *Int. J. Mass Spectrom.* **2001**, *208*, 89–98.

(20) Yang, L.; Sturgeon, R. E. *Anal. Bioanal. Chem.* **2009**, *393*, 377–385.
(21) Yang, L.; Sturgeon, R. E.; Mester, Z.; Meija, J. *Anal. Chem.* **2010**, *82*, 8978–8982.
(22) Wapstra, A. H.; Audi, G.; Thibault, C. *Nucl. Phys. A* **2003**, *729*, 337–676.
(23) Berglund, M.; Wieser, M. E. *Pure Appl. Chem.* **2011**, *83*, 397–410.
(24) Malinovsky, D.; Vanhaecke, F. *Anal. Bioanal. Chem.* **2011**, *400*, 1619–1624.
(25) Buchachenko, A. L. *J. Phys. Chem. A* **2001**, *105*, 9995–10011.
(26) Bigeleisen, J. *J. Am. Chem. Soc.* **1996**, *118*, 3676–3680.
(27) Fontaine, G. H.; Hattendorf, B.; Bourdon, B.; Günther, D. *J. Anal. At. Spectrom.* **2009**, *24*, 637–648.